RESEARCH PAPER

Cancer Biology & Therapy 15:7, 840–850; July 2014; © 2014 Landes Bioscience

Characterization of *LGALS3* (galectin-3) as a player in DNA damage response

Renato S Carvalho[1,2,†], Vanessa C Fernandes[3], Thales C Nepomuceno[3], Deivid C Rodrigues[1], Nicholas T Woods[2], Guilherme Suarez-Kurtz[4], Roger Chammas[5], Alvaro N Monteiro[2], and Marcelo A Carvalho[3,4,*]

[1]Instituto de Biofísica Carlos Chagas Filho; Universidade Federal do Rio de Janeiro; Rio de Janeiro, Brazil; [2]Cancer Epidemiology Program; H. Lee Moffitt Cancer Center & Research Institute; Tampa, FL USA; [3]Instituto Federal do Rio de Janeiro (IFRJ); Rio de Janeiro, Brazil; [4]Programa de Farmacologia; Instituto Nacional de Câncer; Rio de Janeiro, Brazil; [5]Faculdade de Medicina; Universidade de São Paulo; São Paulo, Brazil

[†]Current affiliation: Faculdade de Farmácia; Universidade Federal do Rio de Janeiro; Rio de Janeiro, Brazil

Keywords: DNA damage, galectin-3, BARD1, BRCA1, cancer

Abbreviations: GAL3, galectin-3; DDR, DNA damage repair; HR, homologous recombination; NHEJ, non-homologous end-joining; CRD, carbohydrate recognition domain; tBRCT, BRCT in tandem domain; CyEx, cytoplasmatic extracts; NuEx, nuclear extracts; IP, immunoprecipitation; IB, immunoblotting; MTT, (4,5-dimethylthiazol-2-yl)-2,5-diphenyltetrazolium bromide; IR, ionizing radiation; TAP-MS, tandem affinity purification and mass spectrometry; NT, non-transfected cells

DNA damage repair (DDR) is an orchestrated process encompassing the injury detection to its complete resolution. DNA double-strand break lesions are repaired mainly by two distinct mechanisms: the error-free homologous recombination (HR) and the error-prone non-homologous end-joining. Galectin-3 (GAL3) is the unique member of the chimeric galectins subfamily and is reported to be involved in several cancer development and progression related events. Recently our group described a putative protein interaction between GAL3 and BARD1, the main partner of breast and ovarian cancer susceptibility gene product BRCA1, both involved in HR pathway. In this report we characterized GAL3/BARD1 protein interaction and evaluated the role of GAL3 in DDR pathways using GAL3 silenced human cells exposed to different DNA damage agents. In the absence of GAL3 we observed a delayed DDR response activation, as well as a decrease in the G_2/M cell cycle checkpoint arrest associated with HR pathway. Moreover, using a TAP-MS approach we also determined the protein interaction network of GAL3.

Introduction

DNA damage repair (DDR) is an orchestrated process encompassing the injury detection to its complete resolution. DNA double-strand break lesions are repaired mainly by two distinct mechanisms: the error-free homologous recombination (HR) and the error-prone non-homologous end-joining (NHEJ).[1]

HR is initiated with H2AX phosphorylation by the ATM kinase and the consequent accumulation of several protein complexes, such as Mre11-RAD51-NBS1, at sites of damage.[2] H2AX phosphorylation is also responsible for the recruitment of MDC1, another ATM target, which in turn brings the E3 ubiquitin ligase RNF8 leading to ubiquitination of H2A and H2AX. Ubiquitin chains on these histones are recognized by RAP80, which directs the BRCC36-Abraxas-BRCA1/BARD1 complex to sites of DNA damage.[3,4] BRCA1 is an essential scaffolding protein that participates in many DDR-related processes, such as ionizing radiation sensitivity and cell cycle checkpoint arrest upon damage.[5-7] Several protein interaction modules, including the RING, coiled-coil, and tandem BRCT domains, dictate the scaffolding role of BRCA1.

Galectins are a group of specialized lectins that bind preferentially β-galactosides. Galectin-3 (GAL3) is the unique member of the chimeric galectins subfamily that contains an N-terminal glycine and proline rich domain and a C-terminal carbohydrate recognition domain (CRD).[8] In general, GAL3 exhibits affinity to galactose containing oligosaccharides, such as N-acetyl lactosamine; however, its CRD can also accommodate larger structures, for example polylactosaminoglycans.[9]

Interestingly, GAL3 is normally found in the nucleus of cells, where no galactosides are usually found. Therefore, GAL3 may have distinct functions other than its lectin activity. GAL3 is reported to be involved in several cancer development and progression related events, affecting tumor characteristics such as aggressiveness in breast and thyroid tissues.[10-12] Moreover the response to chemotherapeutic agents was described to be altered in GAL3 silenced cancer cells.[13] However, the molecular mechanisms behind these findings are still poorly understood.

*Correspondence to: Marcelo A Carvalho; Email: marcelo.carvalho@ifrj.edu.br
Submitted: 12/13/2013; Revised: 04/09/2014; Accepted: 04/13/2014; Published Online: 04/22/2014
http://dx.doi.org/10.4161/cbt.28873

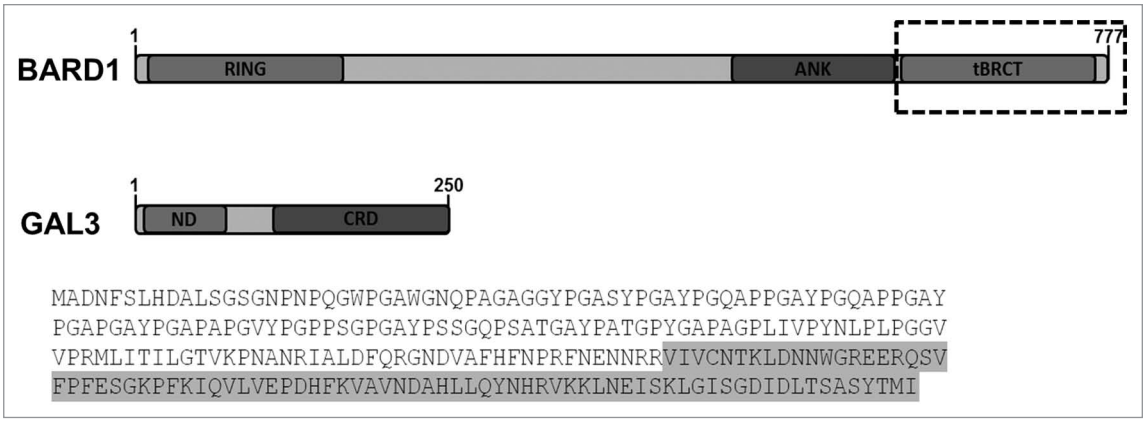

Figure 1. Schematic representation of BARD1 and GAL3. Dotted box depict the BARD1 region described to interact with GAL3. Recognized domains are depicted in dark gray boxes (BARD1: RING, RING finger domain; ANK, ankyrin repeats; tBRCT, tandem BRCT domain. GAL3: ND, N-terminal domain; CRD, carbohydrate recognition domain). GAL3 amino acid sequence is presented with the BARD1 interaction region described by Woods et al. highlighted in gray.

Recently our group described a putative protein interaction between GAL3 and BARD1, the main partner of breast and ovarian cancer susceptibility gene product BRCA1.[14] BARD1 and BRCA1 share structural similarities, bearing an N-terminal RING finger and two C-terminal BRCT in tandem domain (tBRCT).[15] The tBRCT is a common feature in DDR related proteins, found in a small family of 12 proteins that express a total of 15 tandem BRCT domains in the human proteome. The tBRCT is classically described as a reader of specific phosphorylated motifs induced by kinases in response to DNA damage, as ATM, ATR, and DNA-PK.[16,17] However, many protein interactions have also been described with tBRCT domains that do not require phosphorylated ligands.

In this report we evaluated the putative role of GAL3 in DDR pathways using human cells with silenced GAL3 exposed to different DNA damage agents. In the absence of GAL3 we observed a delayed DDR response activation, as well as a decrease in the G_2/M cell cycle checkpoint arrest. Moreover, we characterized GAL3/BARD1 protein interaction, and determined the protein interaction network of GAL3.

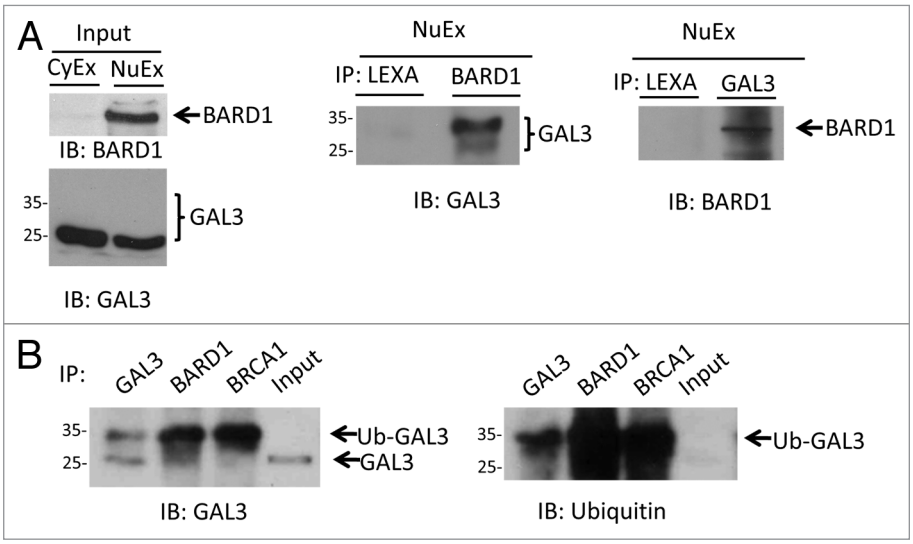

Figure 2. BARD1 and GAL3 interact in mammalian cells. An ubiquitinated form of GAL3 co-exists with the non-modified form and interacts with BARD1 and BRCA1. (**A**) Left panel: GAL3 and BARD1 expression were determined in HeLa cytosolic (CyEx) and nuclear extract (NuEx) by immunoblotting using anti-BARD1 and anti-galectin-3 antibodies. Middle panel: Co-IP assays were performed using HeLa cells NuEx and anti-BARD1 or anti-LexA monoclonal antibodies, immunoblotting was developed using anti-GAL3 antibody. Right panel: Co-IP assays were performed using NuEx and anti-GAL3 or anti-LexA antibodies, immunoblotting was developed using anti-BARD1 antibody. (**B**) Left panel: Co-IP assays were performed using HeLa NuEx using anti-BARD1, anti-BRCA1 or anti-GAL3 antibodies and the subsequent immunoblotting was developed using anti-GAL3. Right panel: Co-IP assays were performed using HeLa NuEx using anti-BARD1, anti-BRCA1, or anti-GAL3 antibodies and the subsequent immunoblotting was developed using anti-ubiquitin antibody.

Results

Galectin-3 and BARD1 interact in mammalian cells

Recently, our group described the tBRCT-protein interaction network for 7 tBRCT domains.[14] Using the BARD1 tBRCT domain as bait, we conducted a yeast-two-hybrid screen and identified a GAL3 fragment (comprising the amino acids residues 170–250, corresponding to its C-terminal region) (**Fig. 1**).

In order to verify this observation we performed co-immunoprecipitations (IP) assays using HeLa nuclear extracts; endogenous GAL3 was co-purified with endogenous BARD1 in forward and reverse immunoprecipitations (**Fig. 2A**). Collectively, these data indicate that GAL3 interacts with BARD1 in human cells.

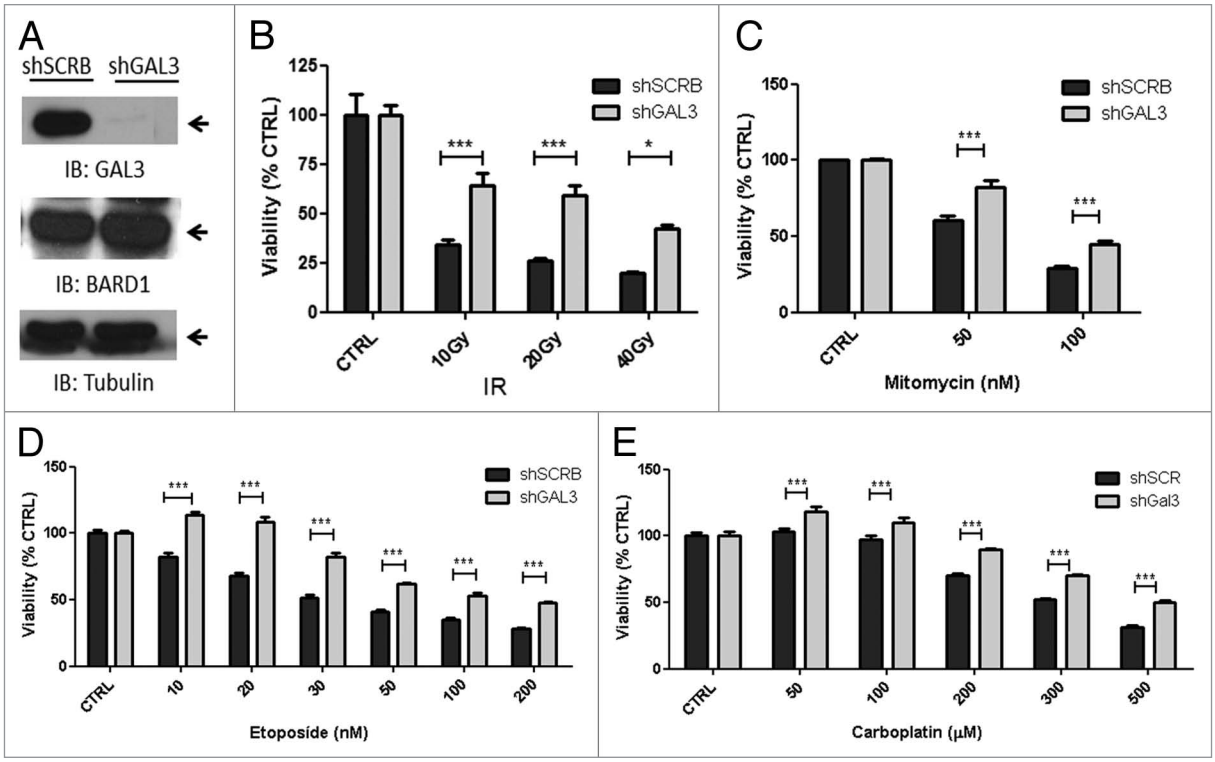

Figure 3. GAL3 silenced cells exhibit increased resistance to DNA damage agents. HeLa cells were silenced using shRNA SCRB (negative control) or shRNA GAL3 and exposed to different DNA damage agents. (**A**) GAL3 and BARD1 expression were determined in HeLa whole cell lysates by immunoblotting using anti-BARD1 and anti-GAL3 antibodies. Tubulin was used as loading control. Silenced cells were exposed to (**B**) IR and incubated for 96 h or (**C**) incubated with different concentrations of Mitomycin C for 96 h, (**D**) etoposide for 48 h, or (**E**) carboplatin for 48 h. After incubation period, cellular viability was assessed by MTT assay. Data are presented as mean ± SD of the viability percentile values relative to untreated cells. *$P < 0.05$, ***$P < 0.001$.

A mono-ubiquitinated form of galectin-3 co-exists with the non-modified form and is found in complexes with BARD1 and BRCA1

As shown in **Figure 2B**, a GAL3 modified form (increased in approximately 9 kDa when compared with the expected MW, 26 kDa) was predominantly observed in association with BARD1. This observation led us to hypothesize that a mono-ubiquitinated form of GAL3 (Ub-GAL3) was enclosed in the same complex with BARD1. Since BRCA1/BARD1 heterodimer has ubiquitin E3 ligase activity, we also investigated the participation of BRCA1 in a complex with GAL3.

To investigate these suppositions, HeLa nuclear extracts were immunoprecipitated using anti-GAL3, anti-BARD1, and anti-BRCA1 antibodies followed by IB detection for GAL3 and ubiquitin. **Figure 2B** shows a prevalent Ub-GAL3 form associated with BARD1 and BRCA1. Curiously, Ub-GAL3 was less abundant than the non-modified form in nuclear extracts, being detected only after being enriched by immunoprecipitation.

***LSGAL3* silenced cells exhibit increased DNA damage resistance**

Since GAL3 was identified in complexes with BARD1 and BRCA1 (**Fig. 2**), and both proteins are known to participate in DDR pathways, we decided to investigate the involvement of GAL3 in these processes. To address this question, HeLa cells were stably silenced for *LGALS3* (shGAL3) and a non-targeting scrambled control (shSCRB). As presented in **Figure 3A**, GAL3 protein levels were nearly undetectable in HeLa shGAL3 whole cell lysates expressing the shGAL3 construct. Noteworthy, BARD1 protein profile was not affected by *LGALS3* silencing when compared with HeLa shSCRB cells (**Fig. 3A**).

Using the stably silenced cell lines, we performed cell viability assays using four different DNA damaging agents: ionizing radiation, etoposide, carboplatin, and mitomycin C. As shown in **Figure 3B**, cells lacking GAL3 expression exhibited an increased resistance to ionizing radiation (10 to 40 Gy). Similarly, statistically significant increases in viability were observed for the three chemotherapeutic agents evaluated in all tested concentrations (**Fig. 3C–E**). It is worth noting that *LGALS3* silenced cells showed up to a 60% increase in viability when compared with shSCRB cells after treatment with 20 nM etoposide (**Fig. 3D**). These data suggest that *LGALS3* plays a role in the cellular response to DNA damage.

***LSGAL3* silenced cells exhibit delayed DDR response**

The increased DNA damage resistance observed in the absence of GAL3 prompted us to evaluate the initial steps in DDR pathway upon IR treatment: the phosphorylation patterns of $ATM^{Ser1981}$ and $H2AX^{Ser139}$ (γH2AX). After treatment with ionizing radiation (10 Gy), ATM phosphorylation was assessed at different time points using HeLa shSCRB or shGAL3 cell lines (**Fig. 4**). As shown in **Figure 4A**, no difference in $ATM^{Ser1981}$ phosphorylation was observed between HeLa shSCRB and shGAL3. Interestingly, this event does not seem to be

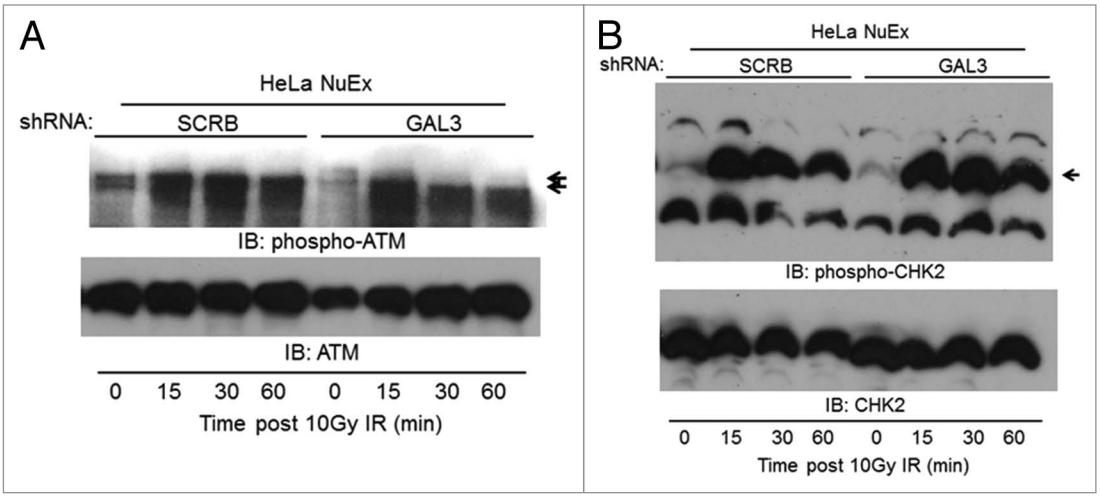

Figure 4. GAL3 silenced cells exhibit altered ATM phosphorylation pattern after DNA damage. GAL3 or SCRB silenced HeLa cells were exposed to IR (10 Gy) and NuEx were obtained after the indicated time intervals. (**A**) ATM and phosphorylated-ATM (Ser[1981]) levels were determined by immunoblotting using specific antibodies. (**B**) CHK2 and phosphorylated-CHK2 (Thr[68]) levels were determined by immunoblotting using specific antibodies.

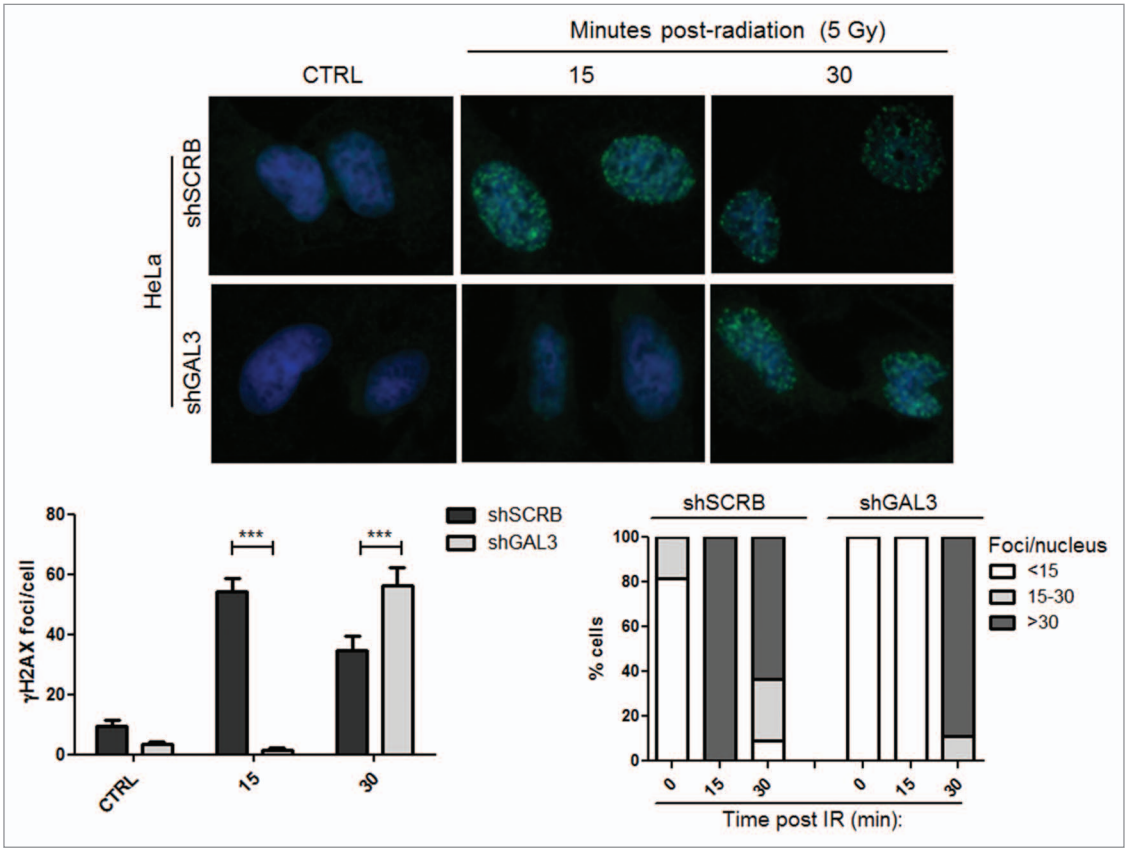

Figure 5. GAL3 silenced cells exhibit delayed phosphorylated-H2AX foci formation after DNA damage. Upper panel: GAL3 or SCRB silenced HeLa cells were exposed to IR (5 Gy) and immunostained after the indicated time intervals using anti-phosphorylated H2AX (Ser[139]). Cells were stained using DAPI. Lower panel: Phosphorylated H2AX (Ser[139]) foci were quantified using Image J software. Data are presented as mean ± SD of absolute foci number/cell. ***$P < 0.001$.

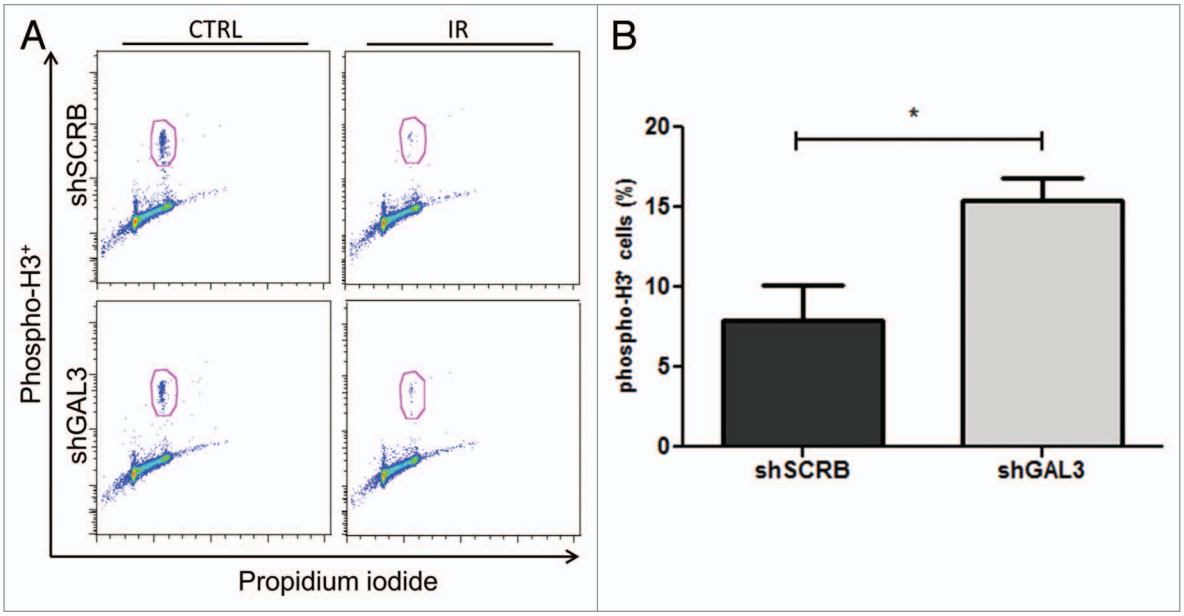

Figure 6. GAL3 silenced cells impaired G_2/M cell cycle arrest after DNA damage. GAL3 or SCRB silenced HeLa cells were exposed to IR (6 Gy) and incubated for 1 h. After recovery period cells were immunostained using anti-phosphorylated H3 (Ser^{28}) and DNA content was stained using PI. (**A**) Representative dot-plots showing DNA content (*x*-axis) and phosphorylated H3 (Ser^{28}) (*y*-axis), depicting the mitotic cell gate (red polygon). (**B**) Quantification of phosphorylated H3 (Ser^{28}) positive cells after DNA damage. Data are presented as mean ± SD, $*P < 0.05$.

directly associated to serine 1981 phosphorylation levels. Both cell lines were able to phosphorylate $ATM^{Ser1981}$ in response to DNA damage; however, at least two different forms of the phosphorylated ATM were observed (**Fig. 4A**, indicated by arrows).

Additionally, CHK2 (another ATM kinase substrate involved in DDR, downstream to H2AX phosphorylation) status was assessed. No major effect was observed in phospho-$CHK2^{Thr68}$ status after DNA damage (**Fig. 4B**).

We next investigated the phosphorylation status of the well-characterized ATM substrate H2AX in different time points upon DNA damage (5 Gy), by quantifying γH2AX foci formation. As shown in **Figure 5**, we observed a delay in γH2AX foci formation in HeLa shGAL3 cell line. Different from HeLa shSCRB IR exposed cells, *LGALS3* silenced cells only exhibited detectable foci 30 min after IR exposure, in contrast to the early (15 min) detectable signal in GAL3-proficient cell line (**Fig. 5**).

Collectively, these results suggest that GAL3 plays a role in the early events in the response to DNA damage but does not affect the activity of ATM or CHK2.

***LSGAL3* silenced cells present an impaired IR-induced G_2/M cell cycle arrest**

The previous observations suggesting a delay in gamma-H2AX focus formation following DNA damage (**Figs. 4 and 5**), prompted us to investigate the GAL3 impact on G_2/M cell cycle checkpoint.

LGALS3 silenced HeLa cells were exposed to IR (6 Gy) and immunostained for phosphorylated histone 3^{Ser10} (phospho-H3), and co-stained with propidium iodide 1 h after the treatment. Flow cytometry analyses were performed to quantify mitotic cells in non-IR and IR exposed conditions. Representative dot-plots are shown in **Figure 6A**.

In response to DNA damage HeLa shSCRB cells displayed a well-characterized G_2/M cell cycle arrest, evidenced by a decrease in the percentage of mitotic cells (7.9 ± 3.7% of total non-irradiated cells, phospho-$H3^+$). HeLa shGAL3 cells also displayed a G_2/M arrest but the extension of this effect was significantly different (15.4 ± 2.5% of total non-irradiated cells, phospho-$H3^+$). As shown in **Figure 6B**, a 2-fold difference was observed in phospho-$H3^+$ *LGALS3* silenced population in comparison to HeLa shSCRB cells after IR, indicating an impaired cell cycle arrest.

GAL3 interacts with DDR pathways-related proteins

To further explore GAL3 biology, we determined its protein interaction network based on TAP assays. The purified proteins were identified by mass spectrometry and were considered putative GAL3 interaction partners only proteins that were not present in control affinity purification. Using this approach, 43 GAL3 protein associations were identified, among them GAL3BP, a well-characterized GAL3 partner, indicating native folding of the ectopic construct (**Table 1**). The identified network includes proteins involved in different biological processes such as cellular component organization, response to chemical stimuli, and developmental processes.

Since GAL3 is a ubiquitous protein, interaction partners were categorized in six protein groups based on subcellular location (plasma membrane, cytoplasm, cytoskeleton, mitochondria, nucleus, and other organelles, **Table 1**). Noteworthy we were able to identify four DDR-related proteins interacting with GAL3, namely PARP1, HSP90AB1, CDC5L, and PRPF19.

Table 1. GAL3 interaction partners identified by TAP-MS

Symbol	Description[a]	Entrez gene ID
Plasma membrane		
ATP1A1	ATPase, Na^+/K^+ transporting, α 1 polypeptide	476
BSG	Basigin (Ok blood group)	682
CADM1	Cell adhesion molecule 1	23705
CCT3	Chaperonin containing TCP1, subunit 3 (gamma)	7203
ITGB1	Integrin, β 1 (fibronectin receptor, β polypeptide	3688
LAMC1	Laminin, gamma 1 (formerly LAMB2)	3915
SLC12A2	Solute carrier family 1 (neutral amino acid transporter), member 5	6558
SLC3A2	Solute carrier family 3 (activators of dibasic and neutral amino acid transport), member 2	6520
Cytoplasm		
AHCY	Adenosylhomocysteinase	191
CKAP4	Cytoskeleton-associated protein 4	10970
DDOST	Dolichyl-diphosphooligosaccharide–protein glycosyltransferase	1650
GLB1	Galactosidase, β 1	2720
HSP90AB1	Heat shock protein 90 kda α (cytosolic), class B member 1	3326
IPO5	Importin 5	3843
KPNB1	Karyopherin (importin) β 1	3837
MYL6	Myosin, light chain 6, alkali, smooth muscle and non-muscle	4637
RPL35	Ribosomal protein L35	11224
RPS20	Ribosomal protein S20	6224
Cytoskeleton		
LAMP2	Lysosomal-associated membrane protein 2	3920
MYH10	Myosin, heavy chain 10, non-muscle	4628
NAP1L1	Nucleosome assembly protein 1-like 1	4673
VIM	Vimentin	7431
Mitochondria		
ATP5C1	ATP synthase, H^+ transporting, mitochondrial F1 complex, gamma polypeptide 1	509
HRNR	Hornerin	388697
MCCC1	Methylcrotonoyl-CoA carboxylase 1 (α)	56922
PDHX	Pyruvate dehydrogenase complex, component X	8050
Nucleus		
ACTA2	Actin, α 2, smooth muscle, aorta	59
CDC5L	Cell division cycle 5-like	988
KIAA1549	KIAA1549	57670
LGALS3BP	Lectin, galactoside-binding, soluble, 3 binding protein	3959
MCCC2	Methylcrotonoyl-CoA carboxylase 2 (β)	64087
MYL12B	Myosin, light chain 12B, regulatory	103910
PARP1	Poly (ADP-ribose) polymerase 1	142
PRPF19	PRP19/PSO4 pre-mRNA processing factor 19 homolog (*S. cerevisiae*)	27339
RPL7A	Ribosomal protein L7A	6130
SLC1A3	Solute carrier family 12 (sodium/potassium/chloride transporters), member 2	6507
SLC1A5	Solute carrier family 1 (glial high affinity glutamate transporter), member 3	6510
TMPO	Thymopoietin	7112

[a]Source: www.genecards.org

Table 1. GAL3 interaction partners identified by TAP-MS (continued)

Symbol	Description[a]	Entrez gene ID
Other organelles		
ECE1	Endothelin converting enzyme 1	1889
NCSTN	Nicastrin	23385
PCCA	Propionyl CoA carboxylase, α polypeptide	5095
RPL12	Ribosomal protein L12	6136
SERPINH1	Serpin peptidase inhibitor, clade H (heat shock protein 47), member 1, (collagen binding protein 1)	871

[a]Source: www.genecards.org

Discussion

Many roles have been suggested for GAL3 in cancer; however, most of them are still to be mechanistically proven.[18] Our group placed GAL3 as a binding partner of the BARD1 tBRCT domain through a wide protein–protein interaction screening. The identified fragment (amino acids 170–250) encompasses the GAL3 CRD sequence that is responsible for the protein glycoconjugate-binding activity (**Fig. 1**).[9,14]

For a long time BARD1 was supposed to be only a BRCA1 accessory, playing a secondary role associated with its N-terminal RING finger domain (responsible to BRCA1/BARD1 heterodimerization). However, BARD1 tBRCT domain (located in its C-terminal) was also proven of functional relevance, depicted by cancer predisposing mutations affecting this domain.[19,20] The BARD1 tBRCT domain is also reported as an interaction domain, mediating protein-protein associations by specific phosphorylated motifs (e.g., pSer-X-X-Phe).[21] Curiously, the sequence Ser-Val-Phe-Pro-Phe-Glu-Ser (amino acids 188–194) found in the identified GAL3 fragment (**Fig. 1**) quite resembles the tBRCT interaction motif. Moreover, an in silico query performed in the PhosphoSitePlus database indicated that both serine residues are prone to phosphorylation in this fragment (pSer-Val-Phe-Pro-Phe-Glu-pSer), suggesting a putative interaction model.[22,23]

The GAL3/BARD1 interaction was confirmed in a endogenous IP approach (**Fig. 2A**), identifying GAL3 as a constitutive component of a BARD1 protein complex and also placing it in a complex with BRCA1 (**Fig. 2B**). It is reasonable to infer that the three proteins were participating in the same complex, but we cannot exclude that GAL3 may take place in two different complexes (**Fig. 2B**). Interestingly, in both situations GAL3 was identified as its monoubiquitinated posttranslational form. According to the PhosphoSitePlus database, at least two independent entries point to an ubiquitination event in GAL3 lysine residue at position 176.

Ubiquitination is not an unusual feature in DDR pathways. In fact, the insertion and recognition of ubiquitinated chains is essential for the correct assembly of the proteins complexes at the DNA damage site, such as the recruitment of RAP80, a member of BRCA1 A complex, via recognition of RNF8-mediated ubiquitination of MDC1.[24] Importantly, BRCA1/BARD1 heterodimer is also an E3 ubiquitin ligase,[25] and since both proteins were able to interact with GAL3, the hypothesis of a direct enzyme/substrate relation cannot be excluded.

Our protein interaction data placed GAL3 at the DDR pathway, due to both BARD1 and BRCA1 interactions. Thus, we investigated the impact of GAL3 silencing in the response to different classes of DNA damage agents; namely IR and etoposide—which promote single strand and mainly double-strand breaks—and the interstrand DNA crosslinking agents cisplatin and mitomycin C (**Fig. 3**). These agents induce the activation of different DNA damage repair mechanisms. DS breaks are resolved by HR and NHEJ, adducts induced by crosslinking are corrected preferentially by nucleotide excision repair, but also with contribution of HR. SS breaks are object of the SS repair pathway that involves APE1, PNKP, TDP1, APTX, and DNA ligases. In addition to the canonical NHEJ pathway, there is an alternative end-joining pathway that utilizes larger stretches of microhomology and engages various factors that also function in HR or SS break repair (MRN complex, PARP1, WRN, LIG1).[26-29]

GAL3 silenced cells exhibited a consistent increase in resistance when treated with damage agents compared with proficient cells (**Fig. 3**). The data suggest a specific role for GAL3 in DDR after injury.

Although most reports correlate GAL3 with anti-apoptotic functions, and thus its overexpression is related to drug resistance,[30] there are evidences also suggesting a pro-apoptotic function for the protein, limited to its nuclear fraction.[31] Curiously, BARD1 exhibited pro-apoptotic potential mediated by its translocation to the mitochondria, an opposing effect to the one described for GAL3 migration to the same organelle. It is plausible to envisage the participation of both a GAL3/BARD1 complex modulating apoptosis control.[32,33]

The HR pathway is a common feature triggered by all tested damage agents. This cascade has many key points such as the activation of ATM. This kinase is auto-phosphorylated upon DNA damage, in particular at the serine residue 1981, and the resulting activated dimers promote the phosphorylation of early events in the HR pathway such as the phosphorylation of histone H2AX, as well as downstream substrates as the CHK2 kinase.[34,35] We investigated the phosphorylation status of both kinases (ATM and CHK2, **Fig. 4**) and also of H2AX (**Fig. 5**), and did not observe differences in the phosphorylation levels of $ATM^{Ser1981}$ or CHK2 after IR treatment. However, GAL3 silenced cells showed a different pattern of $ATM^{Ser1981}$ phosphorylation forms upon DNA damage when compared with proficient cells (**Fig. 4**), suggesting a posttranslational modification leading

to lower MW forms. ATM phosphorylation phenomenon may occur in different sites (not only in Ser1981) and is also associated to different cellular processes, not restricted to the initial DDR signaling. Among these sites, one of particular interest is S794, this residue was found to be linked to apoptosis induction and cell cycle regulation.[36]

Further investigation is required to characterize the altered ATM phosphorylation forms observed in response to IR in GAL3 silenced cells and also explore its eventual association with the observed reduced sensitivity of these cells to DNA damage agents (**Fig. 4**).

The altered ATM phosphorylation pattern upon IR treatment in cells lacking GAL3 expression led us to investigate the kinetics of H2AX phosphorylation (**Fig. 5**). The formation of γH2AX foci is one of the first events in HR cascade, signaling the damaged site to the DDR machinery.[37] γH2AX foci formation is retarded in the absence of GAL3, suggesting an impairment in early steps of HR, involving both ATM and H2AX, but not the downstream element CHK2 (**Figs. 4 and 5**). Curiously, a similar effect on the kinetics of H2AX phosphorylation was reported in PARP1 knockout cells due to a poly-ADP-ribosylation-dependent ATM regulation.[38]

A common cellular response to DNA damage involves the inhibition of cell cycle progression. The impairment of HR key events, such as the observed in BRCA1 deficient cells, is associated to a reduced G_2/M cell cycle arrest, allowing cells to undergo mitosis independently of DNA errors.[39,40] A similar scenario was observed in GAL3 deficient cells in response to IR (**Fig. 6**), suggesting the participation of GAL3 in the DNA damage response pathway.

The DDR is ruled by a sophisticated cellular network that coordinates events requiring actions of various proteins with different functions, from sensoring DNA damage to actual repair.[41] It is reasonable to speculate that the observed delay in γH2AX foci formation and the resistance to DNA damage agents are intrinsic and correlated events, but it is also reasonable to assume an independent participation of GAL3 in two distinct events during DDR. Thus, an eventual pro-apoptotic control performed by GAL3/BARD1 would be abrogated in deficient cells. Recently, a similar scenario was presented by Chen and colleagues, where Gadd45a-deficient cells exhibited an increased resistance to DNA damage associated with a decrease in the apoptosis rate and delayed DNA repair.[42]

In this report we also described a new set of GAL3 protein partners (**Table 1**). Supporting the involvement of GAL3 in DDR, we identified at least four interaction partners that play relevant roles in DNA damage-related events: HSP90AB1, PRPF19, CDC5L, and PARP1.

HSP90 is a chaperone that acts on the correct folding of proteins as CHK1, BRCA2, RAD51, FANCA, DNA-PK, and BRCA1.[43] In response to IR, HSP90 is phosphorylated by DNA-PK, ATR, and ATM kinases, and co-localizes with γH2AX at DNA damage sites. Importantly, cells lacking HSP90 exhibited an impaired maintenance of γH2AX foci, as well as the treatment with HSP90 inhibitors that led to a reduction of BRCA1 protein levels, associated to ubiquitin-proteasome pathway.[43,44]

PRPF19, formerly known as Pso4, was reported to interact with TDT BRCT domain, participating of DNA interstrand crosslinking repair. Moreover, cells lacking PRPF19 expression exhibited an increased sensitivity to IR treatment.[45] PRPF19 also interacts with CDC5L (another novel GAL3 partner, **Table 1**), that is involved in the repair of psoralen-induced DNA crosslinking. This complex also contains the exonuclease WRN which is activated by its association with DNA single strand protein RPA.[46,47] Curiously, PRPF19 contains a U-box domain, associated to E3 ubiquitin ligase activity. Although PRPF19 autoubiquitination was reported, other ubiquitination targets are still to be determined.[48]

PARP1 regulates processes such as gene transcription, apoptosis and DDR, via its poly-ADP ribose conjugating activity.[49] Curiously, this protein encloses a singular BRCT domain and the WGR motif, the latter also found in GAL3, being critical to its self-dimerization.[50,51] Therefore, it is reasonable to speculate that these PARP1 regions may be involved in GAL3 interaction. PARP1 has several substrates, such as histones H1, H2A, and H2B, as well as aurora kinase and p53.[49] It is well described that PARP1 modulates the accumulation of p53 after IR-induced DNA damage.[52] Interestingly, p53 activation induces the downregulation of GAL3 levels in thyroid carcinoma cells, in a HIPK2-dependent mechanism.[53]

Recently, Li and Yu identified BARD1 tBRCT as a poly (ADP-ribose)-binding module and this association is necessary to the proper localization of BRCA1/BARD1 heterodimer to DNA damage sites.[54] Our data suggest the participation of GAL3 in complexes with BRCA1 and BARD1 (and also PARP1), thus, it is reasonable to consider an eventual participation of GAL3 modulating BRCA1/BARD1 heterodimer recruitment to damage sites via its association with PARP1.

Materials and Methods

Cell culture and antibodies

Human HEK293FT cell line was purchased from Invitrogen (Invitrogen, R700-07) and the human cervix adenocarcinoma cell line HeLa was obtained from the Rio de Janeiro Cell Bank (BCRJ, 0100). Both cell lines were maintained in RPMI-1640 (Invitrogen, 22400-089) supplemented with 10% fetal bovine serum (Invitrogen, 16000-044) in 5% CO_2 at 37 °C.

Rabbit anti-BARD1 (Bethyl Laboratories, BL518), mouse anti-galectin-3 (Santa Cruz Biotechnologies, SC5610), and rabbit anti-BRCA1 (Santa Cruz Biotechnologies, SC642) monoclonal antibodies were used for co-immunoprecipitation and immunoblotting. Mouse anti-FLAG (Sigma Co., F1804) and anti-Tubulin (Sigma Co., A2066), rabbit anti-ATM (Millipore, 071286) polyclonal and anti-phospho-ATM^{Ser11981} (Upstate, 05740) monoclonal antibodies, rabbit anti-ubiquitin (Dako Co., Z0458), goat HRP-conjugated anti-mouse Ig (Santa Cruz Biotechnologies, SC2005) and goat HRP-conjugated anti-rabbit Ig polyclonal (Santa Cruz Biotechnologies, SC2301) antibodies were used for IB. Rabbit anti-phospho-H2AX^{Ser139} monoclonal antibody (Cell Signaling, 2577) and goat Alexa Fluor 488 conjugated anti-rabbit

Ig polyclonal antibody (Life Technologies, A11008) were used for immunofluorescence staining. Rat Alexa Fluor 647 conjugated anti-phospho-Histone $H3^{Ser28}$ monoclonal antibody (BD Biosciences, 558217) was used for flow cytometry. All antibodies were used following manufacturer's instructions.

Constructions and transfection

Human Galectin-3 coding sequence was amplified by PCR using the following primers Fw 5′-AAGAATTCAT GGCAGACAAT TTTTCGCTCC-3′ and Rv 5′-AAGGATCCTT ATATCATGGT ATATGAAGCA CTGG -3′ (enclosing EcoRI and BamHI restriction sites, respectively) and the construction pEF-Neo-GAL3 as template.[55] The amplified coding sequence was cloned into pEGFP-C2 (Clontech Laboratories, 6083-1). The same approach was used to generate pNTAP-GAL3 construct, encoding calmodulin binding peptide, streptavidin binding peptide-tagged GAL3. pNTAP-GFP was previously generated by our group.[14]

Transfections were conducted using Fugene6® reagent (Roche, 1988387), following the manufacturer instructions.

Immunoblotting and co-immunoprecipitation

Total cellular extracts were obtained using a mild-RIPA buffer (previously described[56]), supplemented with protein inhibitors cocktail (Sigma Co., P8340). Briefly cells were scraped and incubated on ice with mild-RIPA for 30 min. Cellular debris was removed by centrifugation and the supernatant was collected. Sub-cellular fractionation was performed to obtain cytoplasmatic (CyEx) and nuclear extracts (NuEx) as previously described.[57]

Co-immunoprecipitation (Co-IP) assays were performed by incubating A/G plus agarose beads (Santa Cruz Biotechnologies, SC2003), cellular extracts and the appropriate antibody for 16 h at 4 °C in mild-RIPA buffer, followed by ice-cold mild-RIPA buffer washes.

Immunoblotting (IB) assays were performed as previously described[58] using PVDF membranes (Millipore, PR02531). IBs were developed using a chemiluminescent peroxydase substrate (ECL plus, Amersham Biosciences, RPN2124) followed by autoradiography using Hyperfilm ECL (Amersham, 28906836).

Galectin-3 silencing

Lentiviral particles enclosing pLKO.1 plasmids encoding shRNAs targeting *LGALS3* gene (shGAL3) or a control scramble sequence (shSCRB) were produced in HEK293FT cells using Virapower Lentiviral Expression Kit (Invitrogen, K4975-00). To generate HeLa shGAL3 and HeLa shSCRB, cell lentiviral particles were transduced in HeLa cells, followed by puromycin (Invitrogen, A1113802) selection according to manufacturer instructions.

MTT cell viability assay

Cells were plated in 96-well plates (1×10^6 cells/well), allowed to attach for 24 h, cells were (a) irradiated (10, 20, or 40 Gy) followed by a 96 h recovery period or (b) treated with different chemotherapeutic agents for 48 or 96 h: carboplatin (50–500 μM, Blaüsiegel, B-PLANTIN), etoposide (10–200 nM, Darrow, POSIDON), or mitomycin C (50 and 100 nM, Bristol-Myers-Squib, MUTAMYCIN). Cellular viability was assessed using (4,5-dimethylthiazol-2-yl)-2,5-diphenyltetrazolium bromide (MTT, Sigma Co., M5655), as previously described.[59]

Immunofluorescence assay

Phospho-$H2AX^{Ser139}$ immunofluorescence staining was performed as previously described with slight modifications.[57] Briefly, cells were plated over glass covers slides and allowed to attach for 24 h. Afterwards, cells were exposed to ionizing radiation (IR, 5 Gy), followed by fixation treatment (5 min in formaldehyde 3% v/v and sucrose 2% w/v prepared in PBS) 15, 30, or 60 min post-IR treatment. Cellular membranes were permeabilized and incubated with anti-phospho-$H2AX^{Ser139}$ followed by Alexa Fluor 488-conjugated anti-rabbit Ig secondary antibody. Slides were mounted with Prolong Gold antifade reagent with DAPI (Invitrogen, P-36931). Samples were analyzed by confocal microscopy (Leica, Leica TCS SP5). IR-induced γH2AX foci were quantified using ImageJ software.[60]

Flow cytometry

Early G_2/M checkpoint arrest analysis was performed as previously described.[57] Briefly, HeLa shSCRB and HeLa shGAL3 cells were plated in 6-well plates and allowed to attach for 24 h. Afterwards, cells were exposed to IR (6 Gy) and fixed with ethanol 70% v/v for 4 h. Cells were immunostained with Alexa Fluor 647 conjugated anti-phospho-histone $H3^{Ser28}$ antibody, after then washed with PBS solution and stained with propidium iodide (Sigma Co., 81845) and RNase A (Sigma Co., R4875) solution. Samples were acquired using flow cytometry (BD Biosciences, LRSII) and analyzed with FlowJo v.6.4.7 (TreeStar).

Tandem affinity purification and mass spectrometry (TAP-MS)

GAL3 interacting proteins were identified by TAP-MS assay as previously described.[14] Briefly, HEK293FT cells were transfected with pNTAP-GAL3 or pNTAP-GFP and incubated for 24 h. After this, whole cell lysates were obtained using NETN buffer (Nonidet P40 0,5% v/v, Tris pH8,0 20 mM, NaCl 50 mM, NaF 50 mM, Na_3VO_4 100 mM, DTT 1 mM, PMSF 50 μg/mL). TAP assay was performed using the Interplay Mammalian TAP System (Agilent Technologies, 240107) following manufacturer instruction. The purified proteins were resolved using SDS-PAGE followed by Coomassie blue staining. Stained bands were excised and in-gel trypsin digestion was performed. Eluted protein fragments were separated by nano flow liquid chromatography (Thermo Scientific, U3000) and analyzed by mass spectrometry (Thermo Scientific, LTQ). Protein fragments were identified using Scaffold v.3.2.0 (Proteome Software) and Mascot v.2.2.04 (Matrix Science). The final GAL3 interaction data set consists of proteins identified in pNTAP-GAL3 transfected cells assay, but not in the negative control pNTAP-GFP analysis.

Disclosure of Potential Conflicts of Interest

No potential conflicts of interest were disclosed.

Acknowledgments

The authors would like to acknowledge Fundação de Amparo à Pesquisa do Rio de Janeiro (FAPERJ), CNPQ/INCT Para o Controle do Câncer, and the H. Lee Moffitt Cancer Center and Research Institute Flow Cytometry, Analytical Microscopy and Proteomics Core Facilities.

References

1. Lord CJ, Ashworth A. The DNA damage response and cancer therapy. Nature 2012; 481:287-94; PMID:22258607; http://dx.doi.org/10.1038/nature10760
2. Paull TT, Rogakou EP, Yamazaki V, Kirchgessner CU, Gellert M, Bonner WM. A critical role for histone H2AX in recruitment of repair factors to nuclear foci after DNA damage. Curr Biol 2000; 10:886-95; PMID:10959836; http://dx.doi.org/10.1016/S0960-9822(00)00610-2
3. Lou Z, Minter-Dykhouse K, Franco S, Gostissa M, Rivera MA, Celeste A, Manis JP, van Deursen J, Nussenzweig A, Paull TT, et al. MDC1 maintains genomic stability by participating in the amplification of ATM-dependent DNA damage signals. Mol Cell 2006; 21:187-200; PMID:16427009; http://dx.doi.org/10.1016/j.molcel.2005.11.025
4. Wang B, Elledge SJ. Ubc13/Rnf8 ubiquitin ligases control foci formation of the Rap80/Abraxas/Brca1/Brcc36 complex in response to DNA damage. Proc Natl Acad Sci U S A 2007; 104:20759-63; PMID:18077395; http://dx.doi.org/10.1073/pnas.0710061104
5. Ouchi T, Monteiro AN, August A, Aaronson SA, Hanafusa H. BRCA1 regulates p53-dependent gene expression. Proc Natl Acad Sci U S A 1998; 95:2302-6; PMID:9482880; http://dx.doi.org/10.1073/pnas.95.5.2302
6. Moynahan ME, Cui TY, Jasin M. Homology-directed dna repair, mitomycin-c resistance, and chromosome stability is restored with correction of a Brca1 mutation. Cancer Res 2001; 61:4842-50; PMID:11406561
7. Dapić V, Monteiro AN. Functional implications of BRCA1 for early detection, prevention, and treatment of breast cancer. Crit Rev Eukaryot Gene Expr 2006; 16:233-52; PMID:17073553; http://dx.doi.org/10.1615/CritRevEukarGeneExpr.v16.i3.30
8. Dumic J, Dabelic S, Flögel M. Galectin-3: an open-ended story. Biochim Biophys Acta 2006; 1760:616-35; PMID:16478649; http://dx.doi.org/10.1016/j.bbagen.2005.12.020
9. Knibbs RN, Agrwal N, Wang JL, Goldstein IJ. Carbohydrate-binding protein 35. II. Analysis of the interaction of the recombinant polypeptide with saccharides. J Biol Chem 1993; 268:14940-7; PMID:8325871
10. Honjo Y, Nangia-Makker P, Inohara H, Raz A. Down-regulation of galectin-3 suppresses tumorigenicity of human breast carcinoma cells. Clin Cancer Res 2001; 7:661-8; PMID:11297262
11. Takenaka Y, Inohara H, Yoshii T, Oshima K, Nakahara S, Akahani S, Honjo Y, Yamamoto Y, Raz A, Kubo T. Malignant transformation of thyroid follicular cells by galectin-3. Cancer Lett 2003; 195:111-9; PMID:12767519; http://dx.doi.org/10.1016/S0304-3835(03)00056-9
12. Yoshii T, Inohara H, Takenaka Y, Honjo Y, Akahani S, Nomura T, Raz A, Kubo T. Galectin-3 maintains the transformed phenotype of thyroid papillary carcinoma cells. Int J Oncol 2001; 18:787-92; PMID:11251175
13. Cheong TC, Shin JY, Chun KH. Silencing of galectin-3 changes the gene expression and augments the sensitivity of gastric cancer cells to chemotherapeutic agents. Cancer Sci 2010; 101:94-102; PMID:19843071; http://dx.doi.org/10.1111/j.1349-7006.2009.01364.x
14. Woods NT, Mesquita RD, Sweet M, Carvalho MA, Li X, Liu Y, Nguyen H, Thomas CE, Iversen ES Jr., Marsillac S, et al. Charting the landscape of tandem BRCT domain-mediated protein interactions. Sci Signal 2012; 5:rs6; PMID:22990118; http://dx.doi.org/10.1126/scisignal.2002255
15. Irminger-Finger I, Jefford CE. Is there more to BARD1 than BRCA1? Nat Rev Cancer 2006; 6:382-91; PMID:16633366; http://dx.doi.org/10.1038/nrc1878
16. Scully R, Xie A, Nagaraju G. Molecular functions of BRCA1 in the DNA damage response. Cancer Biol Ther 2004; 3:521-7; PMID:15280660; http://dx.doi.org/10.4161/cbt.3.6.842
17. Mesquita RD, Woods NT, Seabra-Junior ES, Monteiro AN. Tandem BRCT Domains: DNA's Praetorian Guard. Genes Cancer 2010; 1:1140-6; PMID:21533002; http://dx.doi.org/10.1177/1947601910392988
18. Liu FT, Rabinovich GA. Galectins as modulators of tumour progression. Nat Rev Cancer 2005; 5:29-41; PMID:15630413; http://dx.doi.org/10.1038/nrc1527
19. De Brakeleer S, De Grève J, Loris R, Janin N, Lissens W, Sermijn E, Teugels E. Cancer predisposing missense and protein truncating BARD1 mutations in non-BRCA1 or BRCA2 breast cancer families. Hum Mutat 2010; 31:E1175-85; PMID:20077502; http://dx.doi.org/10.1002/humu.21200
20. Alshatwi AA, Hasan TN, Syed NA, Shafi G, Grace BL. Identification of functional SNPs in BARD1 gene and in silico analysis of damaging SNPs: based on data procured from dbSNP database. PLoS One 2012; 7:e43939; PMID:23056176; http://dx.doi.org/10.1371/journal.pone.0043939
21. Thanassoulas A, Nomikos M, Theodoridou M, Yannoukakos D, Mastellos D, Nounesis G. Thermodynamic study of the BRCT domain of BARD1 and its interaction with the -pSER-X-X-Phe-motif-containing BRIP1 peptide. Biochim Biophys Acta 2010; 1804:1908-16; PMID:20451671; http://dx.doi.org/10.1016/j.bbapap.2010.04.012
22. Hornbeck PV, Chabra I, Kornhauser JM, Skrzypek E, Zhang B. PhosphoSite: A bioinformatics resource dedicated to physiological protein phosphorylation. Proteomics 2004; 4:1551-61; PMID:15174125; http://dx.doi.org/10.1002/pmic.200300772
23. Weintz G, Olsen JV, Frühauf K, Niedzielska M, Amit I, Jantsch J, Mages J, Frech C, Dölken L, Mann M, et al. The phosphoproteome of toll-like receptor-activated macrophages. Mol Syst Biol 2010; 6:371; PMID:20531401; http://dx.doi.org/10.1038/msb.2010.29
24. Kolas NK, Chapman JR, Nakada S, Ylanko J, Chahwan R, Sweeney FD, Panier S, Mendez M, Wildenhain J, Thomson TM, et al. Orchestration of the DNA-damage response by the RNF8 ubiquitin ligase. Science 2007; 318:1637-40; PMID:18006705; http://dx.doi.org/10.1126/science.1150034
25. Baer R, Ludwig T. The BRCA1/BARD1 heterodimer, a tumor suppressor complex with ubiquitin E3 ligase activity. Curr Opin Genet Dev 2002; 12:86-91; PMID:11790560; http://dx.doi.org/10.1016/S0959-437X(01)00269-6
26. Jung Y, Lippard SJ. Direct cellular responses to platinum-induced DNA damage. Chem Rev 2007; 107:1387-407; PMID:17455916; http://dx.doi.org/10.1021/cr068207j
27. Lee YJ, Park SJ, Ciccone SL, Kim CR, Lee SH. An in vivo analysis of MMC-induced DNA damage and its repair. Carcinogenesis 2006; 27:446-53; PMID:16258176; http://dx.doi.org/10.1093/carcin/bgi254
28. McClendon AK, Osheroff N. DNA topoisomerase II, genotoxicity, and cancer. Mutat Res 2007; 623:83-97; PMID:17681352; http://dx.doi.org/10.1016/j.mrfmmm.2007.06.009
29. Martin LM, Marples B, Lynch TH, Hollywood D, Marignol L. Exposure to low dose ionising radiation: molecular and clinical consequences. Cancer Lett 2013; 338:209-18; PMID:23693079; http://dx.doi.org/10.1016/j.canlet.2013.05.021
30. Fukumori T, Kanayama HO, Raz A. The role of galectin-3 in cancer drug resistance. Drug Resist Updat 2007; 10:101-8; PMID:17544840; http://dx.doi.org/10.1016/j.drup.2007.04.001
31. Califice S, Castronovo V, Bracke M, van den Brûle F. Dual activities of galectin-3 in human prostate cancer: tumor suppression of nuclear galectin-3 vs tumor promotion of cytoplasmic galectin-3. Oncogene 2004; 23:7527-36; PMID:15326483; http://dx.doi.org/10.1038/sj.onc.1207997
32. Yu F, Finley RL Jr., Raz A, Kim HR. Galectin-3 translocates to the perinuclear membranes and inhibits cytochrome c release from the mitochondria. A role for synexin in galectin-3 translocation. J Biol Chem 2002; 277:15819-27; PMID:11839755; http://dx.doi.org/10.1074/jbc.M200154200
33. Tembe V, Henderson BR. BARD1 translocation to mitochondria correlates with Bax oligomerization, loss of mitochondrial membrane potential, and apoptosis. J Biol Chem 2007; 282:20513-22; PMID:17510055; http://dx.doi.org/10.1074/jbc.M702627200
34. Bakkenist CJ, Kastan MB. DNA damage activates ATM through intermolecular autophosphorylation and dimer dissociation. Nature 2003; 421:499-506; PMID:12556884; http://dx.doi.org/10.1038/nature01368
35. Shiloh Y. ATM and ATR: networking cellular responses to DNA damage. Curr Opin Genet Dev 2001; 11:71-7; PMID:11163154; http://dx.doi.org/10.1016/S0959-437X(00)00159-3
36. Tian B, Yang Q, Mao Z. Phosphorylation of ATM by Cdk5 mediates DNA damage signalling and regulates neuronal death. Nat Cell Biol 2009; 11:211-8; PMID:19151707; http://dx.doi.org/10.1038/ncb1829
37. Podhorecka M, Skladanowski A, Bozko P. H2AX Phosphorylation: Its Role in DNA Damage Response and Cancer Therapy. J Nucleic Acids 2010; 2010; PMID:20811597; http://dx.doi.org/10.4061/2010/920161
38. Haince JF, Kozlov S, Dawson VL, Dawson TM, Hendzel MJ, Lavin MF, Poirier GG. Ataxia telangiectasia mutated (ATM) signaling network is modulated by a novel poly(ADP-ribose)-dependent pathway in the early response to DNA-damaging agents. J Biol Chem 2007; 282:16441-53; PMID:17428792; http://dx.doi.org/10.1074/jbc.M608406200
39. Yarden RI, Pardo-Reoyo S, Sgagias M, Cowan KH, Brody LC. BRCA1 regulates the G2/M checkpoint by activating Chk1 kinase upon DNA damage. Nat Genet 2002; 30:285-9; PMID:11836499; http://dx.doi.org/10.1038/ng837
40. Poehlmann A, Roessner A. Importance of DNA damage checkpoints in the pathogenesis of human cancers. Pathol Res Pract 2010; 206:591-601; PMID:20674189; http://dx.doi.org/10.1016/j.prp.2010.06.006
41. Polo SE, Jackson SP. Dynamics of DNA damage response proteins at DNA breaks: a focus on protein modifications. Genes Dev 2011; 25:409-33; PMID:21363960; http://dx.doi.org/10.1101/gad.2021311
42. Chen Y, Ma X, Zhang M, Wang X, Wang C, Wang H, Guo P, Yuan W, Rudolph KL, Zhan Q, et al. Gadd45a regulates hematopoietic stem cell stress responses in mice. Blood 2014; 123:851-62; PMID:24371210; http://dx.doi.org/10.1182/blood-2013-05-504084
43. Stecklein SR, Kumaraswamy E, Behbod F, Wang W, Chaguturu V, Harlan-Williams LM, Jensen RA. BRCA1 and HSP90 cooperate in homologous and non-homologous DNA double-strand-break repair and G2/M checkpoint activation. Proc Natl Acad Sci U S A 2012; 109:13650-5; PMID:22869732; http://dx.doi.org/10.1073/pnas.1203326109

44. Quanz M, Herbette A, Sayarath M, de Koning L, Dubois T, Sun JS, Dutreix M. Heat shock protein 90α (Hsp90α) is phosphorylated in response to DNA damage and accumulates in repair foci. J Biol Chem 2012; 287:8803-15; PMID:22270370; http://dx.doi.org/10.1074/jbc.M111.320887
45. Mahajan KN, Mitchell BS. Role of human Pso4 in mammalian DNA repair and association with terminal deoxynucleotidyl transferase. Proc Natl Acad Sci U S A 2003; 100:10746-51; PMID:12960389; http://dx.doi.org/10.1073/pnas.1631060100
46. Zhang N, Kaur R, Lu X, Shen X, Li L, Legerski RJ. The Pso4 mRNA splicing and DNA repair complex interacts with WRN for processing of DNA interstrand cross-links. J Biol Chem 2005; 280:40559-67; PMID:16223718; http://dx.doi.org/10.1074/jbc.M508453200
47. Yan H, Toczylowski T, McCane J, Chen C, Liao S. Replication protein A promotes 5′-->3′ end processing during homology-dependent DNA double-strand break repair. J Cell Biol 2011; 192:251-61; PMID:21263027; http://dx.doi.org/10.1083/jcb.201005110
48. Lu X, Legerski RJ. The Prp19/Pso4 core complex undergoes ubiquitylation and structural alterations in response to DNA damage. Biochem Biophys Res Commun 2007; 354:968-74; PMID:17276391; http://dx.doi.org/10.1016/j.bbrc.2007.01.097
49. Krishnakumar R, Kraus WL. The PARP side of the nucleus: molecular actions, physiological outcomes, and clinical targets. Mol Cell 2010; 39:8-24; PMID:20603072; http://dx.doi.org/10.1016/j.molcel.2010.06.017
50. Langelier MF, Planck JL, Roy S, Pascal JM. Structural basis for DNA damage-dependent poly(ADP-ribosyl)ation by human PARP-1. Science 2012; 336:728-32; PMID:22582261; http://dx.doi.org/10.1126/science.1216338
51. Akahani S, Nangia-Makker P, Inohara H, Kim HR, Raz A. Galectin-3: a novel antiapoptotic molecule with a functional BH1 (NWGR) domain of Bcl-2 family. Cancer Res 1997; 57:5272-6; PMID:9393748
52. Valenzuela MT, Guerrero R, Núñez MI, Ruiz De Almodóvar JM, Sarker M, de Murcia G, Oliver FJ. PARP-1 modifies the effectiveness of p53-mediated DNA damage response. Oncogene 2002; 21:1108-16; PMID:11850828; http://dx.doi.org/10.1038/sj.onc.1205169
53. Lavra L, Rinaldo C, Ulivieri A, Luciani E, Fidanza P, Giacomelli L, Bellotti C, Ricci A, Trovato M, Soddu S, et al. The loss of the p53 activator HIPK2 is responsible for galectin-3 overexpression in well differentiated thyroid carcinomas. PLoS One 2011; 6:e20665; PMID:21698151; http://dx.doi.org/10.1371/journal.pone.0020665
54. Li M, Yu X. Function of BRCA1 in the DNA damage response is mediated by ADP-ribosylation. Cancer Cell 2013; 23:693-704; PMID:23680151; http://dx.doi.org/10.1016/j.ccr.2013.03.025
55. Yang RY, Hill PN, Hsu DK, Liu FT. Role of the carboxyl-terminal lectin domain in self-association of galectin-3. Biochemistry 1998; 37:4086-92; PMID:9521730; http://dx.doi.org/10.1021/bi971409c
56. Velkova A, Carvalho MA, Johnson JO, Tavtigian SV, Monteiro AN. Identification of Filamin A as a BRCA1-interacting protein required for efficient DNA repair. Cell Cycle 2010; 9:1421-33; PMID:20305393; http://dx.doi.org/10.4161/cc.9.7.11256
57. Rios-Doria J, Velkova A, Dapic V, Galán-Caridad JM, Dapic V, Carvalho MA, Melendez J, Monteiro AN. Ectopic expression of histone H2AX mutants reveals a role for its post-translational modifications. Cancer Biol Ther 2009; 8:422-34; PMID:19305155; http://dx.doi.org/10.4161/cbt.8.5.7592
58. Laemmli UK. Cleavage of structural proteins during the assembly of the head of bacteriophage T4. Nature 1970; 227:680-5; PMID:5432063; http://dx.doi.org/10.1038/227680a0
59. Mosmann T. Rapid colorimetric assay for cellular growth and survival: application to proliferation and cytotoxicity assays. J Immunol Methods 1983; 65:55-63; PMID:6606682; http://dx.doi.org/10.1016/0022-1759(83)90303-4
60. Schneider CA, Rasband WS, Eliceiri KW. NIH Image to ImageJ: 25 years of image analysis. Nat Methods 2012; 9:671-5; PMID:22930834; http://dx.doi.org/10.1038/nmeth.2089